Paul Shreve
David W. Townsend
Editors

Clinical PET-CT in Radiology

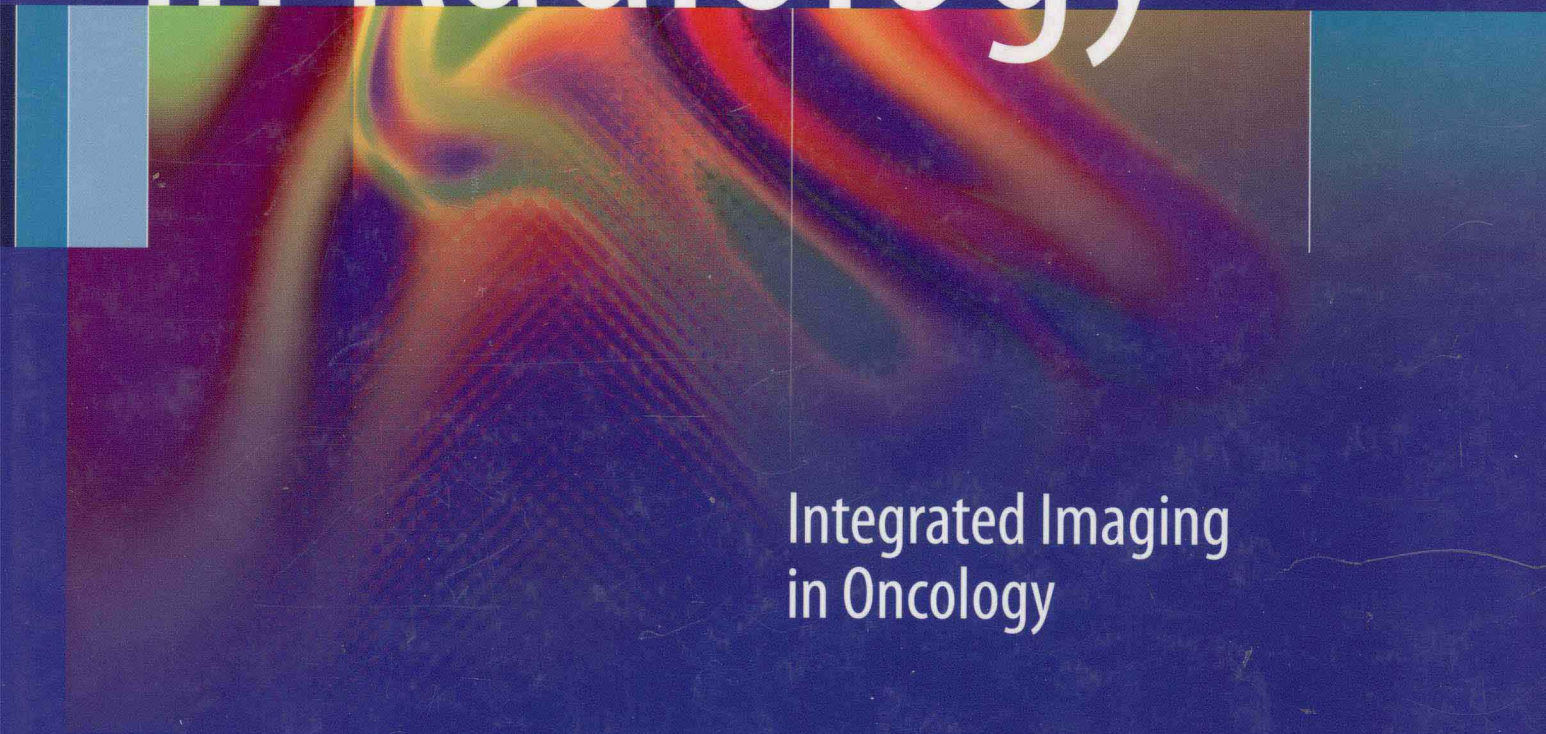

Integrated Imaging in Oncology

Springer

Paul Shreve · David W. Townsend
Editors

Clinical PET-CT in Radiology

Integrated Imaging in Oncology

Springer

Editors
Paul Shreve
Advanced Radiology Services
Grand Rapids, MI
USA
pshreve@earthlink.net

David W. Townsend
Head, PET and SPECT Development
Singapore Bioimaging Consortium
Singapore
david_townsend@sbic.a-star.edu.sg

ISBN 978-0-387-48900-1 e-ISBN 978-0-387-48902-5
DOI 10.1007/978-0-387-48902-5
Springer New York Dordrecht Heidelberg London

Preface

It has been nearly a decade since the first PET-CT scanners became commercially available. At the time of the initial launch of clinical PET-CT scanners it was thought at most 30% of the PET scanner market would be in the form of PET-CT scanners. Within only a few years (by 2006), however, PET-CT scanners replaced stand-alone PET scanners completely in commercial offerings, and today over 5,000 PET-CT scanners have been delivered worldwide. The remarkably rapid adoption of PET-CT is not entirely surprising, as the overwhelming clinical application of PET-CT has been body oncology imaging, and the merging of the anatomic and metabolic information provided by CT and FDG PET scans was a natural and already ongoing practice for body oncology imaging.

The original intent of PET-CT was to provide clinical CT and clinical PET in one scan procedure with the images sets inherently registered and aligned to facilitate interpretation of both modalities. The notion of merging the anatomic information of CT with the metabolic information of PET was suggested by a cancer surgeon in the early 1990s, but in fact the practice of integrating the interpretation of complimentary imaging modalities for clinical diagnosis has been ongoing in disease-based or organ system-based medical imaging subspecialties. This trend has accelerated recently with the widespread application of PACs and teleradiology as well as continued refinements in image registration and image fusion software. The acceptance of PET-CT hybrid scanners has more recently led to commercial SPECT-CT hybrid scanners and to the tentative development of PET-MRI scanners; the concept of hybrid imaging and multimodality imaging diagnosis is a broad and pervasive process occurring in medical imaging.

Since the introduction of commercial PET-CT scanners, published textbooks have approached the subject mainly from a nuclear medicine perspective, including applications to neurologic and cardiac imaging, and discussion of PET radiotracers other than FDG. The true necessity of the hybrid scanner applies to body imaging and in particular the vast majority of applications of clinical PET-CT today remain in body oncology imaging. In this textbook we bring together all aspects of PET-CT relevant to clinical body oncology imaging using clinical CT and clinical FDG PET. The intent is to provide practicing imaging physicians with both a comprehensive and practical text, which treats PET-CT as an integrated anatomic-metabolic medical imaging procedure applied to cancer imaging that it currently is, and was always intended to be. Ample coverage of the relevant physics and clinical oncology is included for reference. The physics and instrumentation chapters are oriented to provide an overview of the available technology and some of the physical concepts without entering into excessive detail. The clinical chapters are structured to provide concise and structured background regarding the clinical management of each cancer and the role of PET-CT imaging in all phases of patient management. It is assumed the reader has some background in both PET and CT interpretation. The intent of each clinical chapter is to help the imaging physician more completely understand the relationship and role of the integrated modality imaging with respect to the overall treatment of the cancer patient. We hope that this text will be a valuable companion for the imaging physician and further establish PET-CT in the mainstream of cancer imaging.

David Townsend, Ph.D.
Singapore

Paul Shreve, M.D.
Grand Rapids, Michigan

Contributors

Harry Agress Jr. M.D.
Chairman, Department of Radiology, Hackensack University Medical Center, Hackensack NJ, USA

Gerald Antoch, M.D.
Professor, Department of Diagnostic and Interventional Radiology, University Hospital Essen, Essen, Germany

Suzanne L. Aquino, M.D.
Consultant, NightHawk Radiology Services, Scottsdale AZ, USA

Thomas Beyer, Ph.D.
Professor, Department of Nuclear Medicine, University Hospital Essen, Essen, Germany and cmi-experts GmbH Zurich, Switzerland

Michael Blake, M.D., B.Sc., MRCPI, FFR (RCSI), FRCR
Director of Abdominal PET-CT, Department of Abdominal Imaging and Intervention, Massachusetts General Hospital, Boston MA, USA

Todd M. Blodgett, M.D.
Assistant Professor, President, FRG Molecular Imaging, Department of Radiology, University of Pittsburgh Medical Center, Foundation Radiology Group, Pittsburgh PA, USA

Andreas Bockisch, M.D., Ph.D.
Director, Clinic and Policlinic for Nuclear Medicine, Department of Nuclear Medicine, University Hospital Essen, Essen, Germany

Trond Velde Bogsrud, M.D.
Researcher, Department of Diagnostic Imaging, Division of Nuclear Medicine, University Clinic, The Norwegian Radium Hospital/Rikshospitalet University Hospital, Montebello Oslo, Norway

Barton F. Branstetter, IV M.D.
Associate Professor, Director, Head and Neck Imaging, Clinical Director of Neuroradiology, Departments of Radiology, Otolaryngology and Biomedical Informatics, University of Pittsburgh Medical Center, Pittsburgh PA, USA

Jacqueline Brunetti, M.D.
Associate Clinical Professor, Medical Director, Department of Radiology, Columbia University College of Physicians and Surgeons, Holy Name Hospital, Teaneck NJ, USA

Carlos A. Buchpiguel, M.D., Ph.D.
Associate Professor, Director PET-CT Laboratory, Department of Radiology, São Paulo University School of Medicine, Hospital do Coração, São Paulo, Brazil

Chuong Bui, MBBS, FRACP
Clinical Lecturer, Medicine, Staff specialist, Nepean Clinical School, Nuclear Medicine Department, Nepean Hospital, The University of Sydney, NSW, Australia

Jonathan P.J. Carney, Ph.D.
Assistant Professor, Department of Radiology, University of Pittsburgh Medical Center, Pittsburgh PA, USA

Natalie Charnley, MBChB, MRCP, FRCR
Researcher, University of Manchester Wolfson Molecular Imaging Centre, Preston, Lanchester, United Kingdom

Gary J.R. Cook, MBBS, M.Sc., M.D., FRCR, FRCP
Consultant Nuclear Medicine Physician, Department of Nuclear Medicine and PET, Royal Marsden Hospital, Surrey, United Kingdom

Thomas F. DeLaney, M.D.
Associate Professor, Medical Director, Department of Radiation Oncology, Harvard Medical School, Northeast Proton Therapy Center, Massachusetts General Hospital, Boston MA, USA

Sukru Mehmet Erturk, M.D.
Associate Professor, Department of Radiology, Sisli Etfal Training and Research Hospital, Istanbul, Turkey

James W. Fletcher, M.D.
Professor, Director, Division of Nuclear Medicine/PET, Director, PET Imaging Center, Division of Nuclear Medicine/PET, Department of Radiology, Indiana/Purdue University, Indiana University School of Medicine, Indianapolis IN, USA

Michael M. Graham, M.D., Ph.D.
Professor, Department of Radiology-Nuclear Medicine, University of Iowa, Iowa City IA, USA

Ian D. Hay, M.D., Ph.D.
Professor, Section of Endocrinology, Department of Internal Medicine, Mayo Clinic, Rochester MN, USA

Terry Jones, D.Sc., F Med Sci
Professor, The PET Research Advisory Company, Cheshire, United Kingdom

Laurie B. Jones-Jackson, M.D.
Assistant Professor of Clinical Radiology & Radiological Sciences, Vanderbilt University Medical Center, Nashville TN, USA

Joseph J. Junewick, M.D.
Chairman, Department of Radiology, Spectrum Health Hospitals, Grand Rapids, Advanced Radiology Services, PC, Grand Rapids Division, Grand Rapids MI, USA

Marc Kachelrieß, Dipl.-Phys
Professor, Department of Medical Imaging, Institute of Medical Physics (IMP), University of Erlangen Nuremberg, Erlangen, Germany

Mannudeep Kalra, MBBS, M.D., DNB
Director of MGH, Department of Radiology, Center for Evaluation of Radiologic Technologies, Massachusetts General Hospital, Boston MA, USA

Lale Kostakoglu, M.D.
Professor, Section of Nuclear Medicine, Department of Radiology, Mt. Sinai Medical Center, New York, NY, USA

Vikram Krishnasetty, M.D.
Private Practice, Columbus Radiology Corporation, Columbus OH, USA

Hilmar Kuehl, M.D.
Senior Physician, Department of Diagnostic and Interventional Radiology, University Hospital Essen, Essen, Germany

Steven Kymes, Ph.D., MHA
Research Assistant Professor, Department of Ophthalmology and Visual Sciences, Washington University School of Medicine, St. Louis MO, USA

Val J. Lowe, M.D.
Professor, Department of Radiology, Division of Nuclear Medicine, Mayo Clinic, Rochester MN, USA

Carolyn Cidis Meltzer, M.D.
Associate Dean for Research, Professor and Chair, Department of Radiology, School of Medicine, Emory University Hospital, Emory University School of Medicine, Atlanta GA, USA

Marisa H. Miceli, M.D.
Resident, Department of Internal Medicine, Oakwood Hospital and Medical Center, Dearborn MI, USA

Sanjay Paidisetty, BS
Intern, Department of Radiology, University of Pittsburgh Medical Center, Pittsburgh PA, USA

Edwin L. Palmer, M.D.
Associate Radiologist, Nuclear Imaging – Division of Molecular Imaging & PET-CT, Massachusetts General Hospital, Boston MA, USA

Pat Price, M.D., FRCP, FRCR
Professor, Imaging Department, Imperial College, London, United Kingdom

Robert E. Reiman, MSPH, M.D.
Assistant Clinical Professor, Radiation Safety Division, Duke University Medical Center, Durham NC, USA

Dushyant Sahani, M.D.
Medical Director of CT Services, Department of Abdominal Imaging and Intervention, Massachusetts General Hospital, Boston MA, USA

James A. Scott, M.D.
Associate Professor, Department of Radiology, Massachusetts General Hospital, Boston MA, USA

Anthony F. Shields, M.D., Ph.D.
Professor of Medicine and Oncology, Department of Internal Medicine, Karmanos Cancer Institute, Wayne State University, Detroit MI, USA

Paul Shreve, M.D.
Advanced Radiology Services, P.C., Michigan State University College of Human Medicine, Spectrum Health Lemmen-Holten Cancer Center, Grand Rapids MI, USA

James Slattery, MRCPI, FFR (RCSI), FRCR
Fellow, Division of Abdominal Imaging and Interventional Radiology,
Massachusetts General Hospital, Boston MA, USA

Nancy M. Swanston, CNMT, PET, RT(N)
Manager, Diagnostic Imaging, Division of Diagnostic Imaging, The University
of Texas M.D., Anderson Cancer Center, Houston TX, USA

Mark Tann, M.D.
Associate Professor of Clinical Radiology, Department of Radiology and Imaging Sciences,
Indiana University School of Medicine, Indianapolis IN, USA

Rick Tetrault, CNMT, RT(N), PET
Administrative Director of Imaging Services, Department of Radiology, Dana-Farber Cancer
Institute, Boston MA, USA

David W. Townsend, Ph.D.
Head, PET and SPECT Development, Singapore Bioimaging Consortium, Singapore

Timothy G. Turkington, Ph.D.
Associate Professor, Department of Radiology and Department of Biomedical Engineering,
Duke University and Duke University Medical Center, Durham NC, USA

Annick D. Van den Abbeele, M.D.
Chief, Founding Director, Department of Imaging, Center for Biomedical Imaging
and Oncology, Dana-Farber Cancer Institute, Boston MA, USA

Patrick Veit, M.D.
Radiologist, Department of Diagnostic and Interventional Radiology,
University Hospital Essen, Germany

Ronald C. Walker, M.D., FACNM
Professor, Clinical Radiology & Radiological Sciences, Vanderbilt University Medical
Center, Nashville TN, USA

Yat Yin Yau, MBBS (OLD), FHKCR, FHKAM
Associate Professor, Director, Diagnostic Imaging, Nuclear Medicine and PET-CT,
Department of Radiology, University of Hong Kong, Hong Kong Adventist Hospital,
Hong Kong, China

Contents

Chapter 1
Principles, Design, and Operation of Multi-slice CT

Marc Kachelriess

Major technical improvements in CT have been taken place since its introduction in 1972 by Godfrey N. Hounsfield (Fig. 1.1). Even in daily clinical routine whole-body CT scans with isotropic submillimeter resolution within a single breath-hold are available. The high spatial resolution combined with volumetric imaging enables CT angiography (CTA) and virtual endoscopy to be performed. In addition CT's high temporal resolution in combination with dedicated image reconstruction algorithms provides superb images of the heart with few motion artifacts.

True 3D data acquisition became available with the introduction of spiral CT in 1989 by W.A. Kalender [1–3]. Spiral CT requires the scanner to rotate continuously and acquire data continuously. During the spiral scan the patient is translated through the CT gantry. Relative to the patient the focal spot and the detector move along a spiral or helical trajectory (Fig. 1.2). The symmetry of the scan trajectory allows for an arbitrary and retrospective selection of the longitudinal image position (z-position). The continuous axial sampling is required for high-quality 3D displays and led to a renaissance of CT [3].

As an enhancement to single-slice spiral CT (SSCT) multi-slice spiral CT (MSCT) scanners became available in 1998. They further improve the scanner's volume coverage, z-resolution, and scan speed. For example, typical chest exams are carried out with collimations of 1 × 5 mm in 36 s with single-slice, 4 × 1 mm in 30 s with 4-slice, and 16 × 0.75 mm in 10 s with 16-slice scanners. Today, even 64 × 0.5 mm scans rotating with up to three rotations per second can be used (see Fig. 1.2).

This chapter is an introduction to the basics of clinical CT. It covers technological issues such as tube and detector design, image reconstruction algorithms, as well as special techniques such as cardiac CT or dynamic CT. The reader will further get an overview of the relations between image quality and dose and will become familiar with dose reduction methods that are provided by the manufacturers as well as dose reduction techniques that can be readily applied to optimize scan protocols.

M. Kachelriess (✉)
Department of Medical Imaging, Institute of Medical Physics,
University of Erlangen Nuremberg, Henkestr. 91,
Erlangen 91052, Germany
e-mail: marc.kachelriess@imp.uni-erlangen.de

Basic CT Principles

From radiography we know that the information available from a single projection is limited. The information can be increased by taking two projections, typically anteroposterior and lateral. However, the radiographic images still show a superposition of all the objects that have been irradiated. Further increasing the number of projection directions (views) is of little help since the observer is not able to mentally solve the superposition problem and to "reconstruct" the internal information of the object (Fig. 1.3).

Fortunately it can be shown that a complete reconstruction of the object's interior is mathematically possible as long as a large number of views have been acquired over an angular range of 180° or more. This acquisition scheme is implemented in computed tomography scanners by using an x-ray tube that rotates around the patient. On the opposing side of the x-ray tube a cylindrical detector consisting of about 10^3 channels per slice is mounted (Figs. 1.2 and 1.4). The shape of the x-ray ensemble is called a fan-beam when the detector consists of only few slices and is called cone-beam when the detector approaches an area detector. During a full rotation 10^3 readouts of the detector are performed per detector slice. Altogether about 10^6 intensity measurements are taken per slice and rotation.

Physically, x-ray CT is the measurement of the object's x-ray absorption along straight lines. For I_0 incident quanta and an object layer of thickness d and attenuation coefficient μ the number I of quanta reaching the detector is given by the exponential attenuation law as

$$I = I_0 e^{-\mu d}.$$

The negative logarithm p of each intensity measurement I gives us information about the product of the object attenuation and

P. Shreve and D.W. Townsend (eds.), *Clinical PET-CT in Radiology: Integrated Imaging in Oncology*,
DOI 10.1007/978-0-387-48902-5_1, © Springer Science+Business Media, LLC 2011

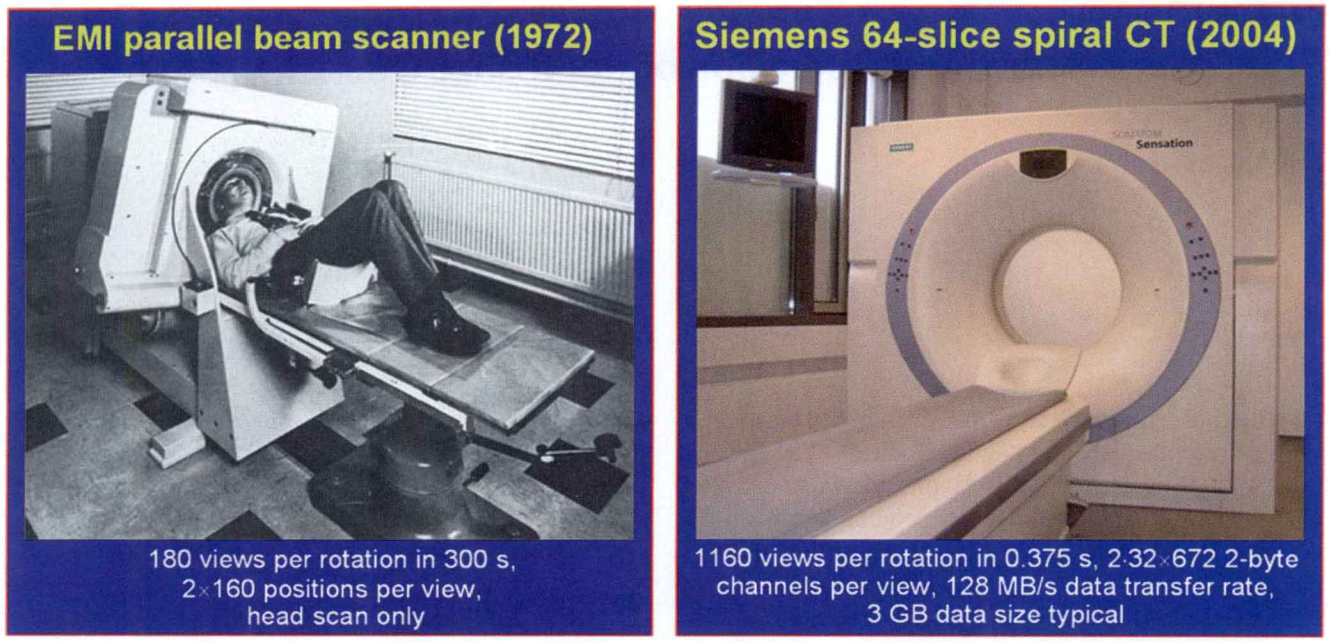

Fig. 1.1 Today, subsecond true 3D cone-beam scans with submillimeter spatial resolution and 50–100 ms temporal resolution are routinely available

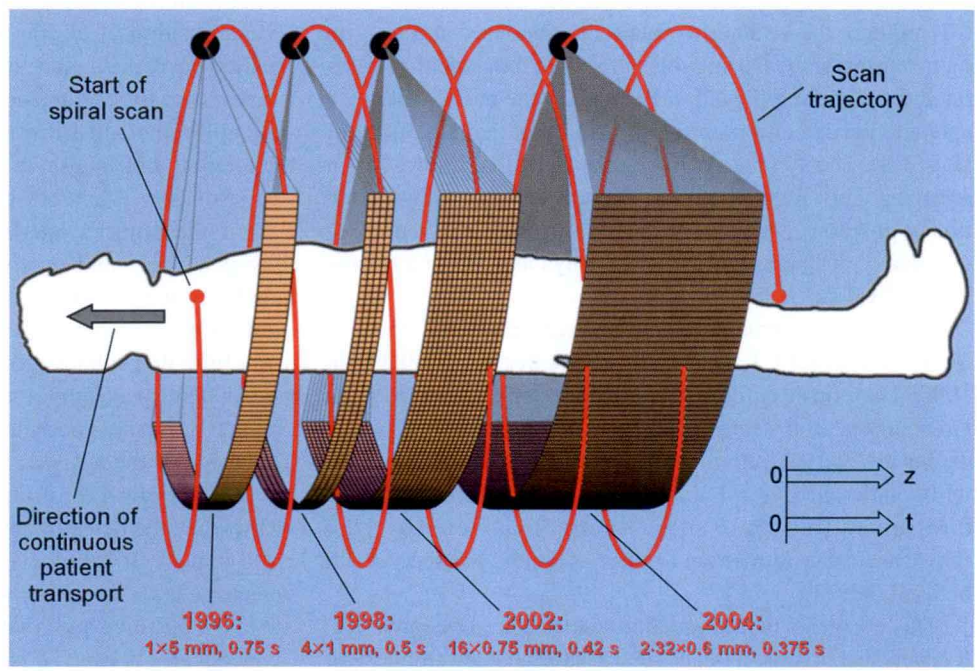

Fig. 1.2 Spiral CT scan principle and four generations of CT scanners. The collimation is given in the form $M \times S$, with M being the number of simultaneously acquired slices and S being the collimated slice thickness

thickness. For nonhomogeneous objects the attenuation coefficient is a function of x, y, and z. Then, the projection value p corresponds to the line integral along line L of the object's linear attenuation coefficient distribution $\mu(x, y, z)$:

$$P(L) = -In\frac{I(L)}{I_0} = \int_L dL\mu(x, y, z)$$

I_0 is the primary x-ray intensity and is needed for proper normalization. It is proportional to the tube current.

We are interested in obtaining knowledge of $\mu(x, y, z)$ by reconstructing the acquired data $p(L)$. The process of computing the CT image $f(x, y, z)$ – the CT image is an accurate approximation to $\mu(x, y, z)$ – from the set of measured projection

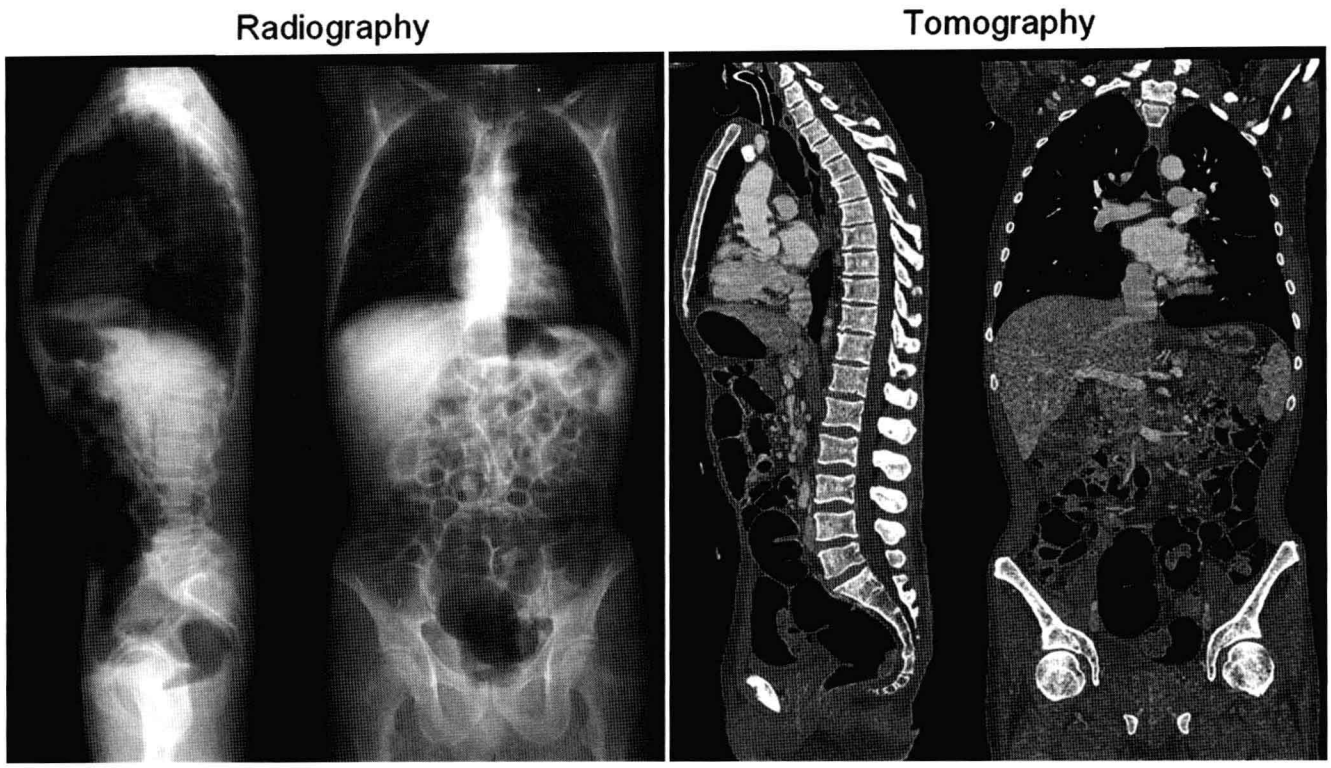

Fig. 1.3 Radiography provides only limited information due to the superpositioned information of several objects. Typically, only one or two projections are acquired. CT, in contrast, allows one to derive the complete volumetric information from a very large number of projections

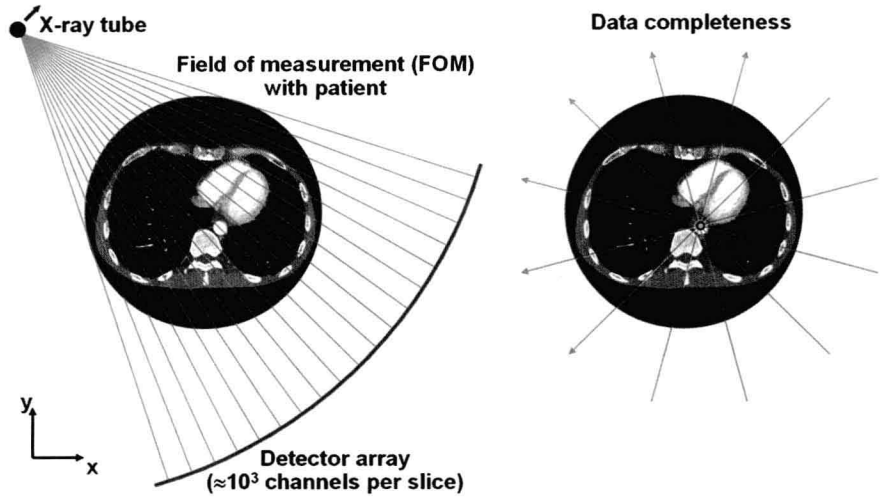

Fig. 1.4 X-ray CT is the measurement of x-ray photon attenuation along straight lines. An object point can be reconstructed as long as it has been viewed by the x-rays under an angular interval of 180° or more. If this applies to all object points within the field of measurement the data are said to be complete

values *p(L)* is called *image reconstruction* and is one of the key components of a CT scanner. For single-slice CT scanners images can be reconstructed slice-by-slice and image reconstruction is rather simple. It consists of a filtering of the projection data with the reconstruction kernel followed by a backprojection into image domain and can be formulated as

$$f(x,y) = \int_0^{\pi} \mathrm{d}\vartheta p(\vartheta,\xi) * k(\xi)\big|_{\xi = x\cos\vartheta + y\sin\vartheta}.$$

This so-called filtered backprojection (FBP) is implemented in all clinical CT scanners. Several reconstruction kernels $k(\xi)$ are available to allow image sharpness (spatial resolution) and image noise characteristics to be modified.

The image values $f(x,y,z)$ are converted into CT values prior to storage by applying the linear function

$$CT = \frac{f - \mu_{\text{water}}}{\mu_{\text{water}}} 1{,}000\,HU.$$

where HU stands for Hounsfield units. The relation is based on the requirement that air (zero attenuation) has a CT value of −1,000 HU and water has a value of 0 HU. The CT values have been introduced by Hounsfield to replace the μ values by an integer quantity. We can interpret the CT value of a pixel or voxel as being the density of the object relative to the density of water at the respective location. For example, 200 HU means that the object density at that location is 1.2 times the density of water. An illustration of the CT scale is shown in Fig. 1.5. CT values range from −1,000 to 3,000 HU except for very dense materials such as dental fillings or metal implants.

CT images are usually displayed as grayscale images. The mapping from CT values to gray values can be controlled by the user to optimize contrast. In CT the display window is usually parameterized by the center C and width W. Values between $C-W/2$ and $C+W/2$ are linearly mapped to the gray values ranging from black to white, whereas values below and above that "window" are displayed black and white, respectively (Fig. 1.6). For example, the window (0, 600) means that it is centered at 0 HU and has a width of 600 HU. Thus, values in the range from −300 HU to 300 HU are mapped to the gray values; values below −300 HU are displayed black and values above 300 HU are displayed white.

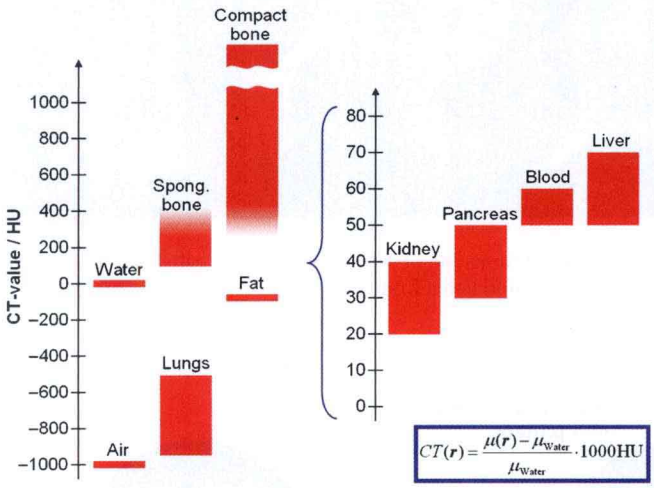

Fig. 1.5 Ranges of CT values of the most important organs

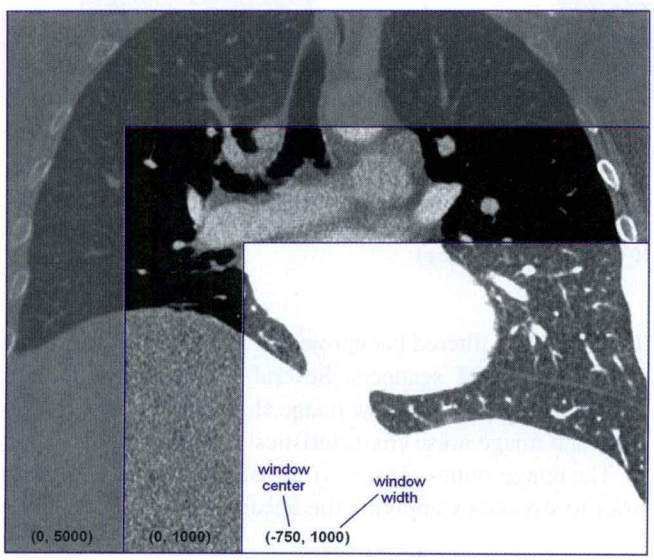

Fig. 1.6 CT image of the thorax displayed with three different window settings

CT Design

A clinical CT scanner consists of the patient table, the gantry, the reconstruction, and viewing PCs and a cooling system. The main purpose of the patient table is to move the patient through the gantry during the scan. Only then can complete anatomic regions be acquired. Further, the table's vertical degree of freedom allows it to be lowered until the patient can comfortably lie down. The gantry comprises a stationary part and a rotational part. Power and data are transferred via slip rings. Continuous rotation and continuous data acquisition are supported. The components carried by the gantry are the x-ray tube and the x-ray detector.

Two kind of tubes are in use today. A typical x-ray tube consists of a vacuum-filled tube envelope. Inside the vacuum is the cathode and a rotating anode with one bearing Fig. 1.7 (*left*). This conventional concept has the disadvantage that tube cooling is inefficient and that the one-sided bearing cannot tolerate high forces. It is also difficult to lubricate bearings in a vacuum. To improve these conventional tubes, vendors try to maximize the heat capacity (expressed in mega heat-units, or MHU) to minimize cooling delays. Recently, a new CT tube has become available where the cathode, the anode, and the envelope together rotate in the cooling medium Fig. 1.7 (*right*). Due to the direct contact to the cooling oil, there is no need to store the heat and thus there will be no cooling delays [4].

Data transfer rate limitations imply a restriction on the number of slices that can be read out simultaneously. Often, scans with fast rotation time acquire fewer slices than scans with slower rotation times. One therefore distinguishes between the number of detector rows that are built into a detector and the number of slices M that can be read out simultaneously. Obviously, the number of slices M is the critical parameter for the user, and not the number of detector rows. Electronic combination (binning) of neighboring rows is used to generate thicker collimated slices and to make use of all detector rows available. An example of modern detector technology is shown in Fig. 1.8. The adaptive array technology has a higher x-ray sensitivity and requires less patient dose than the matrix array detectors since binning to lower spatial resolution includes less detector gaps (septa) with adaptive detectors than

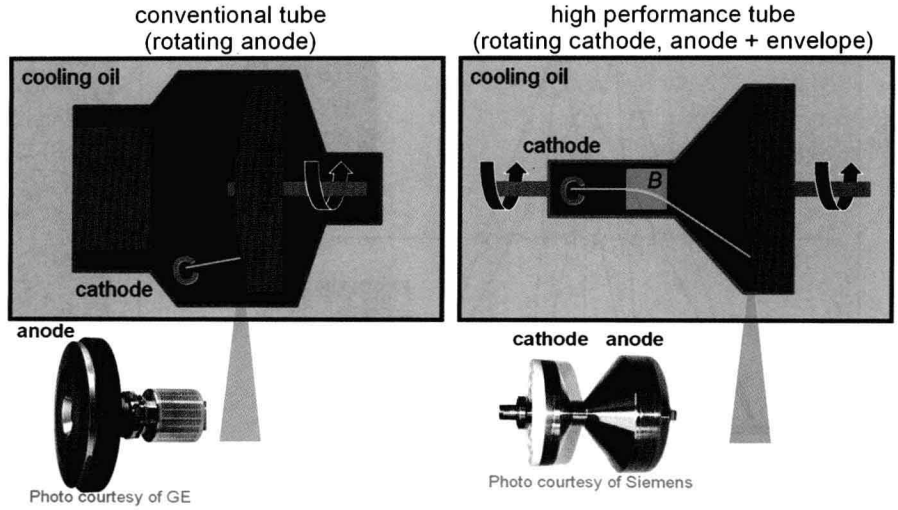

Fig. 1.7 Conventional x-ray tube versus rotating envelope technology (courtesy General Electric, Piscataway, NJ; and Siemens, Munich, Germany)

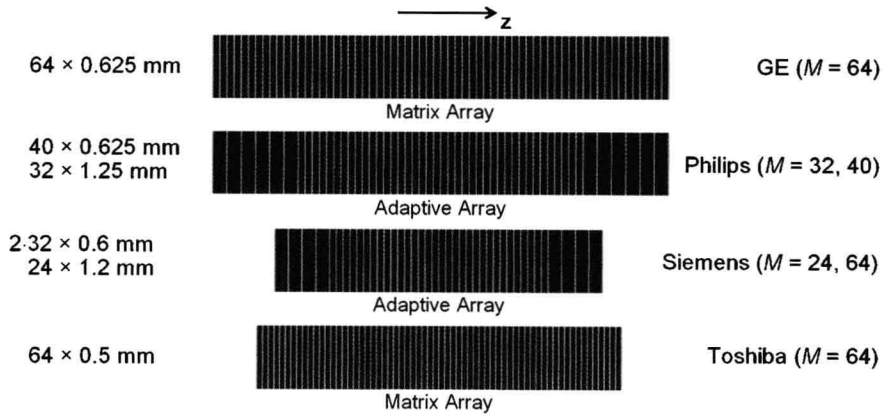

Fig. 1.8 Detector concepts available in 2004. Due to a flying focal spot that jumps back and forth in the longitudinal direction the Siemens detector allows to acquire 64 slices while it provides only 32 high resolution detector rows. It is the only scanner that fulfills the Nyquist sampling criterion in the z-direction

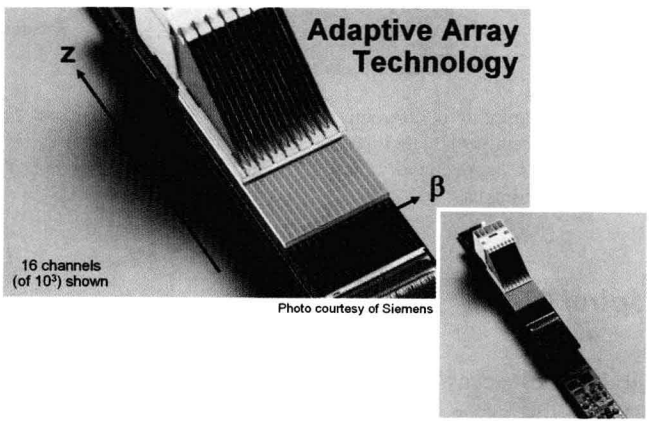

Fig. 1.9 Photo of a 40-row 64-slice adaptive array detector (courtesy Siemens, Munich, Germany)

with matrix detectors. A photo of a typical 64-slice detector is shown in Fig. 1.9; data transfer rates of up to 300 MB per second are achieved with such a system.

The Siemens Sensation 64 scanner has a distinctive feature that allows 64 slices to be acquired from only 32 rows: the z-flying focal spot (zFFS). Between two adjacent readings the focal spot jumps back and forth on the tube anode (a few thousand times per second) to double the sampling distance. Slices of 0.6 mm thickness are acquired at a sampling distance of 0.3 mm (Fig. 1.10). This so-called double sampling, that fulfills the Nyquist sampling condition, improves spatial resolution and reduces spiral windmill artifacts [5].

Advanced CT Principles

Before a CT scan can be started the acquisition software must register the patient. Basic information that is required are the patient name, patient age (birth date), and patient sex. Then, the patient is placed on the table. If required, contrast injection is prepared, ECG leads are applied, spirometric devices are attached, or other preparations are done. Often, the patient is instructed how to behave during the scan to be prepared for the breath-hold commands. In parallel, scan protocols can be selected and scan parameters can be modified.

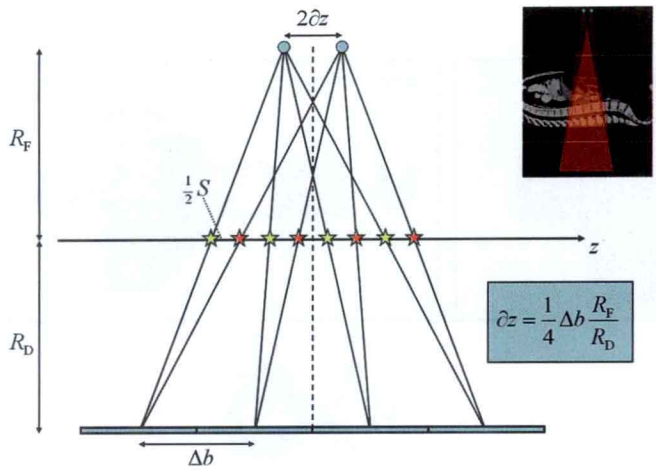

Fig. 1.10 Illustration of the zFFS. Double sampling is indicated by the yellow and red stars

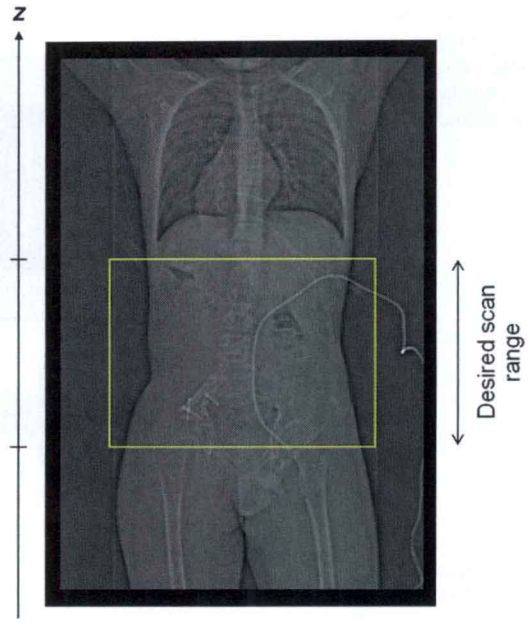

Fig. 1.11 The topogram is a digitally enhanced version of a radiographic projection used to graphically select the desired scan range

Topogram

Most CT scans start by acquiring an overview radiographic image of the patient. This is done by stopping the gantry rotation and by moving the table through the gantry during data acquisition. The image obtained is known as the topogram, the scanogram, or the scout view (Fig. 1.11). It mainly serves to determine the final CT scan range. This is done by the placement of one or more rectangular ROIs that define the z-positions of scan start and end for one or more scans of the same patient. Internally, the scanner may further utilize the topogram information to compute a patient specific tube current control curve that will be used during the scan (see below).

Conventional CT

Before the introduction of spiral CT a CT scan consisted of a rotation about the stationary object followed by a translation of the patient by one slice thickness (for today's multi-slice scanners the scan increment is M times the slice thickness). This scan mode is called conventional CT or step-and-shoot CT, and we may also refer to the combination of several circle scans as a sequence scan or a sequential scan.

Image reconstruction for sequence scans is fairly easy since each slice can be reconstructed separately using filtered backprojection. There are two major drawbacks in conventional CT. First, step-and-shoot scans are rather slow due to the interscan delay when shifting the patient. Second, z-sampling is rather inadequate and there is no true longitudinal translation invariance. This means that scan results may randomly depend on the absolute location of objects, especially for thick slices (Fig. 1.12).

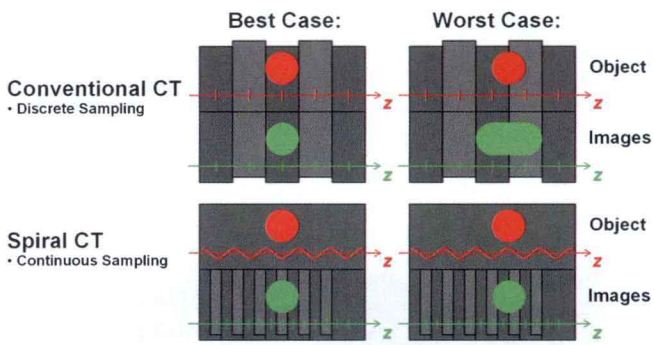

Fig. 1.12 Sampling in conventional CT is sparse, and objects may be imaged differently when their position relative to the slice center varies. This may not happen with spiral CT scans where sampling in z is (almost) continuous

Spiral CT

Today, most scans are carried out in spiral mode. In the late 1980s, just after continuously rotating scanners became available, this scan mode was introduced by Willi A. Kalender [1–3]. It performs continuous data acquisition while the patient moves at constant speed through the gantry (cf. Fig. 1.2). To obtain high-quality images the z-interpolation is required as an additional image reconstruction step. Given a desired reconstruction position z_R the z-interpolation uses projection data acquired at positions adjacent to that plane to synthesize virtual scan data corresponding to a circular scan at $z = z_R$ (Fig. 1.13). Typically, but not necessarily, linear